Supplementary Information for

Enterobactin- and salmochelin-β-lactam conjugates induce cell morphologies consistent with inhibition of penicillin-binding proteins in uropathogenic *Escherichia coli* CFT073

Artur Sargun[1], Timothy C. Johnstone[1], Hui Zhi[2], Manuela Raffatellu[2-4], and Elizabeth M. Nolan[1,*]

[1]Department of Chemistry, Massachusetts Institute of Technology, Cambridge, MA 02139

[2]Division of Host-Microbe Systems and Therapeutics, Department of Pediatrics, University of California San Diego, La Jolla, CA 92093

[3]Center for Microbiome Innovation, University of California San Diego, La Jolla, CA 92093

[4]Chiba University-UC San Diego Center for Mucosal Immunology, Allergy, and Vaccines, La Jolla, CA 92093

*Corresponding author: lnolan@mit.edu

Phone: 617-452-2495

This Supplementary Information includes:

Supplementary Experimental

Supplementary Tables

Supplementary Schemes

Supplementary Figures

Supplementary Experimental

Construction of the *E. coli* CFT073 *fepA iroN ihA* mutant

The *fepA iroN ihA* triple mutant of *E. coli* CFT073 (Table S1) was constructed using the λ Red recombinase system.[1] The λ Red recombinase encoding plasmid pJK611 (pKD46::*sacB*; temperature-sensitive) was transformed into electrocompetent *E. coli* MSC216 cells (*iroN fepA* mutant). Primers homologous to sequences flanking the 5′ and 3′ ends of the target genes were used to amplify a chloramphenicol (Cm^R, from pKD3)[1] resistance gene. (H1P1-iha-CFT: GGCAACGTATTCTACCGTCAGTGATAGCGTT-TTGTTATTAGTGTAGGCTGGAGCTGCTTC; H2P2-iha-CFT: TGTATTGTCTTGCC-GGTTAACATGATCGGAGATTAGTAATCATATGAATATCCTCCTTA). To replace the selected gene with a resistance cassette, the amplicons were transformed into electrocompetent *E. coli* MSC216 (pJK611) grown in LB medium supplemented with L-arabinose to induce λ Red expression. Finally, colonies were incubated at 42°C to remove the temperature-sensitive pJK611 plasmid from the cells. To confirm integration of the resistance cassette and deletion of the target, mutant strains and wild-type controls were each assayed using three PCR amplifications (5' end, 3' end, deleted target). Primers that flank the target sequence (iha-upF: AATGTTTCTATCAGTATTCG; iha-dnR: AACGTCACTCTCT-CTGTAAAC) were used together or in conjunction with common test primers (Cm-seqF: TAATATCCAGCTGAACGGTCTGG; Cm-seqR ATGGGCAAATATTATACGC) for the Cm cassette to test and sequence for the deleted target and both new-junction fragments.

Supplementary Tables

Table S1. Bacterial strains employed in this study

Strain or plasmid	Relevant characteristics or genotype	Source or reference
E. coli K-12	Common lab strain, non-pathogenic	[3]
E. coli CFT073	Clinical isolate, UPEC	ATCC
MSC 206	CFT073 Δ*fepA*::kan (Kan^R)	[6]
MSC 219	CFT073 Δ*iroN*::*tetRA* (Tet^R)	[6]
MSC 228	CFT073 Δ*fepC*::kan (Kan^R)	[6]
MSC 230	CFT073 Δ*fepDG*::kan (Kan^R)	[6]
MSC 216	CFT073 Δ*fepA*::kan Δ*iroN*::*tetRA* (Kan^R Tet^R)	[6]
HZE125	CFT073 Δ*fepA*::kan Δ*iroN*::*tetRA* Δ*iha*::Cm (Kan^R Tet^R Cm^R)	This work
E. coli UTI89	Clinical isolate, UPEC	[7]
E. coli ATCC 35218	Class A serine β-lactamase producer	ATCC
S. aureus ATCC 25923	Clinical isolate, pathogenic Standard laboratory test strain	ATCC

Table S2. Iron content of growth media as determined by ICP-MS[a]

Growth medium	[Fe] (μM)
LB	6.44
	6.12
50% MHB	4.81
	4.75
Modified M9	0.33
	0.35

[a] The values measured for two representative samples from each medium are given.

Table S3. Characterization of Compounds **1-6**

Compound	Analytical HPLC R_t, min[a]	Observed *m/z*[b]	Calculated *m/z*[b]	Yield, mg (%)
Ent-Amp, **1**	17.5	1379.4054[c]	1379.4026[c]	2.1 (64)
DGE-Amp, **2**	15.5	1681.5223	1681.5263	1.7 (40)
Ent-Lex, **3**	18.1	1377.3903[c]	1377.3870[c]	2.2 (66)
DGE-Lex, **4**	15.2	1701.4914[c]	1701.4926[c]	2.9 (70)
Ent-Mem, **5**	16.0	1413.4470[c]	1413.4445[c]	1.4 (41)
DGE-Mem, **6**	13.2	1715.5646	1715.5682	2.2 (52)

[a] HPLC gradient used for all compounds is 0% B for 5 min (column equilibration) followed by 0-100% B over 30 min, 1 mL/min. [b] All *m/z* values correspond to the $[M+H^+]$ species unless noted otherwise. [c] *m/z* values correspond to the $[M+Na^+]$ species.

Table S4. Minimum inhibitory concentration (MIC) of the Ent/DGE-β-lactam conjugates

Strain	**MIC (M)**								
	Amp	**Ent-Amp 1**	**DGE-Amp 2**	**Lex**	**Ent-Lex 3**	**DGE-Lex 4**	**Mem**	**Ent-Mem 5**	**DGE-Mem 6**
E. coli									
K12	10^{-5}	10^{-8}	$>10^{-5}$	$>10^{-5}$	10^{-5}	$>10^{-5}$	10^{-7}	10^{-8}	$>10^{-5}$
UTI89	10^{-5}	10^{-7}	10^{-7}	$>10^{-5}$	10^{-5}	10^{-5}	10^{-7}	10^{-8}	10^{-8}
ATCC 35218	10^{-5}	$>10^{-5}$	$>10^{-5}$	$>10^{-5}$	$>10^{-5}$	$>10^{-5}$	10^{-7}	10^{-8}	$>10^{-5}$
CFT073	10^{-5}	10^{-8}	10^{-8}	$>10^{-5}$	10^{-5}	10^{-5}	10^{-7}	10^{-8}	10^{-8}
CFT073 *fepA*	10^{-5}	10^{-7}	10^{-7}	$>10^{-5}$	10^{-5}	10^{-5}	10^{-7}	10^{-8}	10^{-8}
CFT073 *iroN*	10^{-5}	10^{-8}	10^{-5}	$>10^{-5}$	10^{-5}	10^{-5}	10^{-7}	10^{-8}	10^{-5}
CFT073 *fepA iroN*	10^{-5}	10^{-5}	10^{-5}	$>10^{-5}$	$>10^{-5}$	10^{-5}	10^{-7}	10^{-5}	10^{-5}
CFT073 *fepA iroN iha*	10^{-5}	10^{-5}	10^{-5}	$>10^{-5}$	10^{-5}	10^{-5}	10^{-7}	10^{-5}	10^{-5}
CFT073 *fepC*	10^{-5}	10^{-8}	10^{-8}	$>10^{-5}$	10^{-6}	10^{-6}	10^{-7}	10^{-7}	10^{-7}
CFT073 *fepDG*	10^{-5}	10^{-8}	10^{-8}	$>10^{-5}$	10^{-6}	10^{-6}	10^{-7}	10^{-7}	10^{-7}
S. aureus									
ATCC 25923	10^{-6}	10^{-5}	$>10^{-5}$	10^{-6}	10^{-5}	$>10^{-5}$	10^{-7}	$>10^{-5}$	$>10^{-5}$

Supplementary Schemes

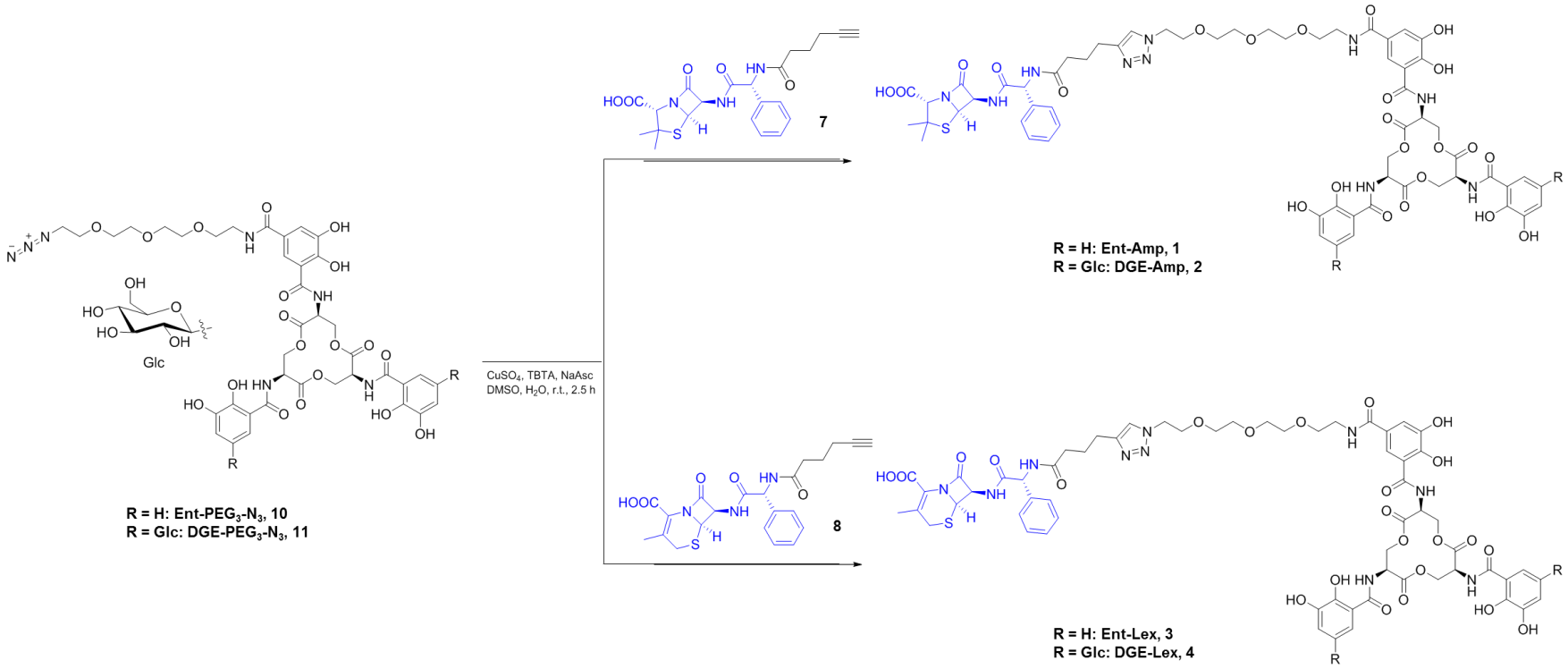

Scheme S1. Synthesis of Ent/DGE-Amp **1, 2** and Ent/DGE-Lex **3, 4** conjugates. The curved line on the β-glycosidic bond of glucose (Glc) represents the point of attachment to the catechol.

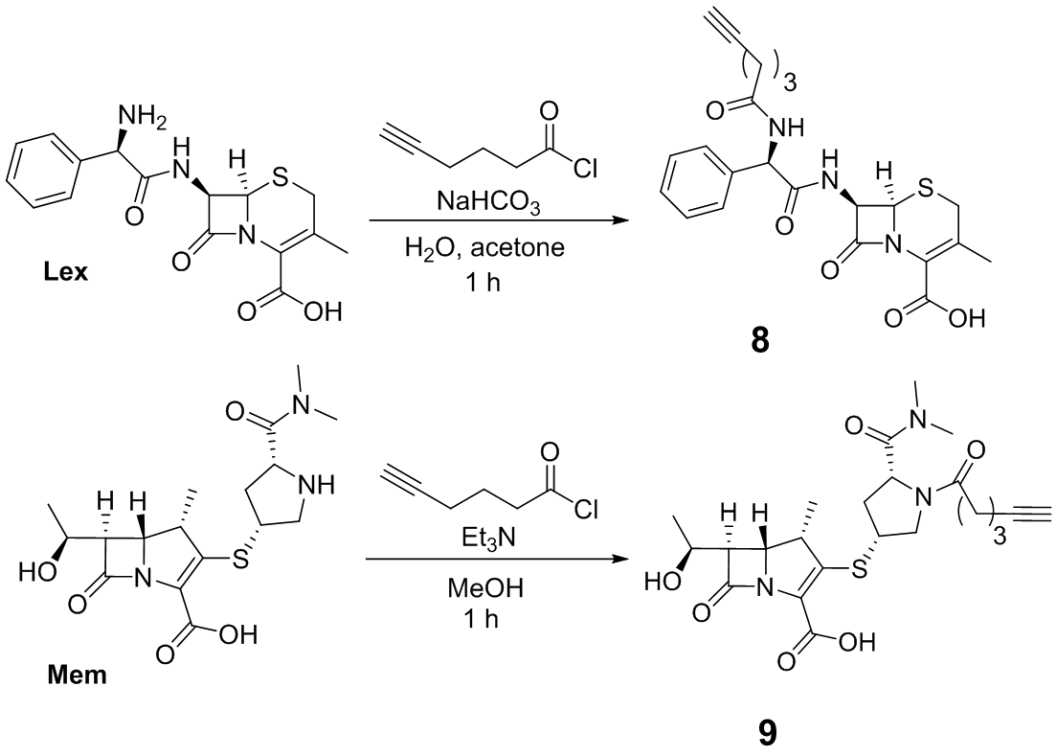

Scheme S2. Synthesis of the Lex- **8** and Mem-alkynes **9**.

Supplementary Figures

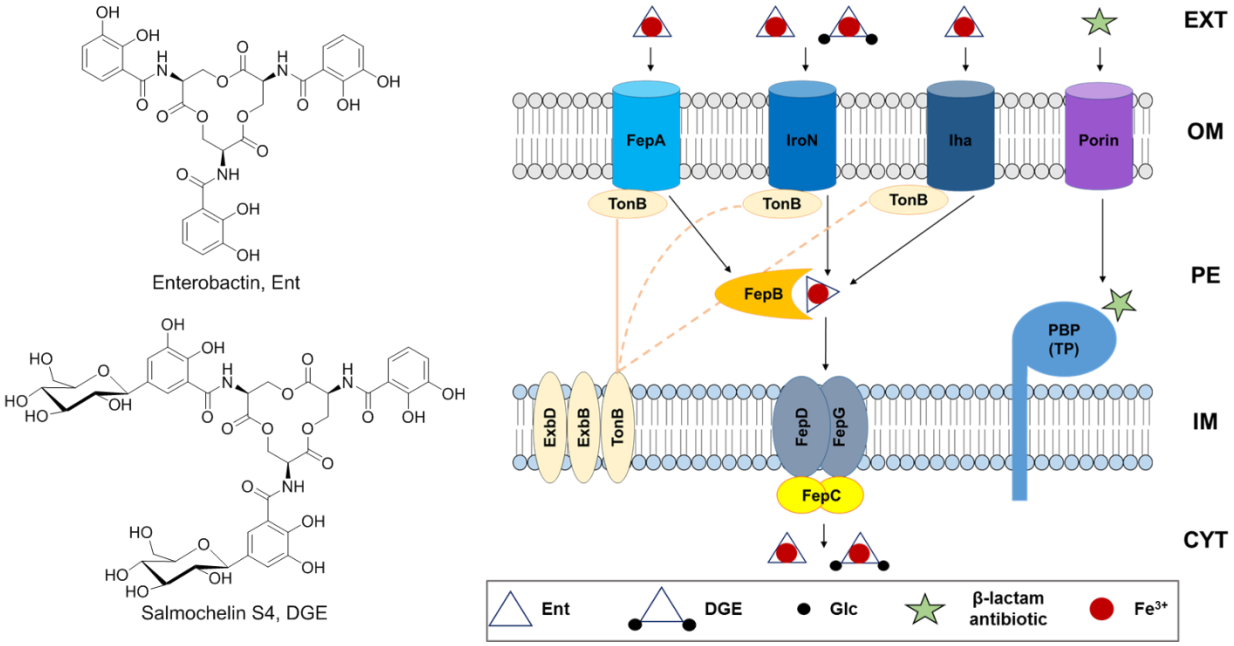

(a) (b)

Figure S1. (a) The chemical structure of enterobactin (Ent) and salmochelin S4 (diglucosylated Ent, DGE); (b) cartoon depiction of the Ent and DGE transport and processing machinery in *E. coli*; Glc, glucose. The external environment (EXT), outer membrane (OM), periplasm (PE), inner membrane (IM), and cytoplasm (CYT) are given at the right. The transpeptidase domain (TP) of a penicillin-binding protein (PBP) is shown for simplicity. The FepA, IroN, and Iha OM receptors are powered by three individual TonB-ExbB-ExbD complexes (only one TonB-ExbB-ExbD complex is shown for clarity). Lipopolysaccharides and peptidoglycan omitted for simplicity.

Enterobactin (Ent) (**Figure S1a**) is a *tris*-catecholate siderophore produced by Gram-negative species including *E. coli*, *Salmonella enterica* and *Klebsiella pneumoniae*.[8,9] The high iron-binding affinity of Ent (K_a ~ 10^{49} M^{-1})[10,11] allows bacteria to scavenge Fe^{3+} from the host environment and form $[Fe(Ent)]^{3-}$.[12] In *E. coli,* $[Fe(Ent)]^{3-}$ is recognized by the OM receptors FepA, IroN and Iha (*E. coli* CFT073)[13–15] and is transported into the periplasm utilizing the energy provided by the TonB-ExbB-ExbD complex (**Figure S1b**). The periplasmic-binding protein FepB carries $[Fe(Ent)]^{3-}$ to the inner membrane (IM), where the ATP-binding cassette (ABC) transporter FepCDG relays the Fe^{3+}-siderophore into the cytoplasm. Subsequent processing by enterobactin esterases results in hydrolysis of the trilactone ring, which facilitates iron release.

Several Ent producers also biosynthesize salmochelins, C-glucosylated analogs of Ent. For instance, salmochelin S4, named herein diglucosylated Ent (DGE), is a C5, C'5-diglucosylated analogue of Ent.[16] DGE is deployed by bacteria to acquire iron and evade the Ent-scavenging host-defense protein lipocalin-2.[17–20] The C-glucosyltransferase (IroB) required for glucosylation of Ent is encoded by the pathogen-associated *iroA* gene cluster (*iroBCDEN*),[21–23] along with additional transport proteins (IroCN) and hydrolase enzymes (IroDE). The OM transporter IroN (**Figure S1b**) transports $[Fe(DGE)]^{3-}$ into the periplasm.[14]

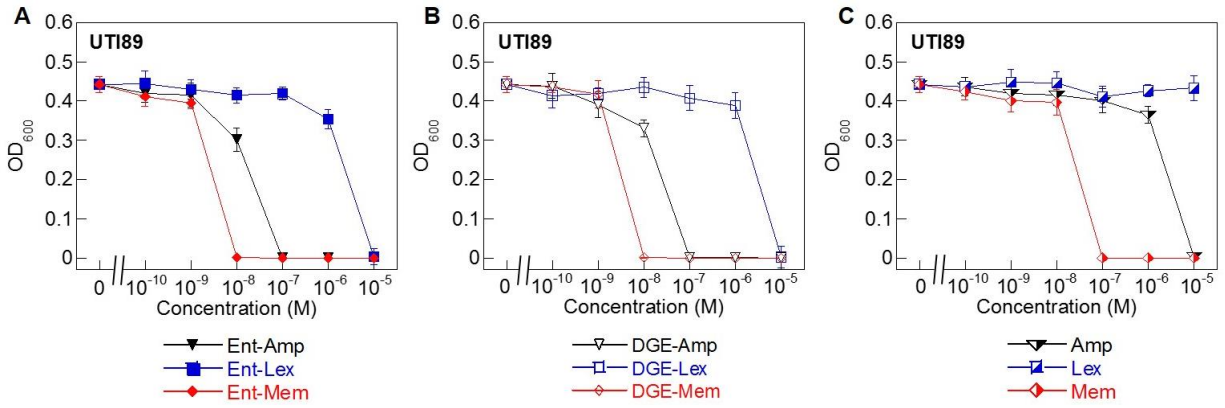

Figure S2. Antibacterial activity of Ent/DGE-β-lactam conjugates **1**-**6** against uropathogenic *E. coli* UTI89. (A) Activity of Ent-Amp/Lex/Mem **1**, **3**, and **5**; (B) activity of DGE-Amp/Lex/Mem **2**, **4**, and **6**; (C) activity of the parent antibiotics Amp, Lex and Mem. All assays were performed in modified M9 medium (20 h, 30°C; mean ± standard deviation, *n* = 3).

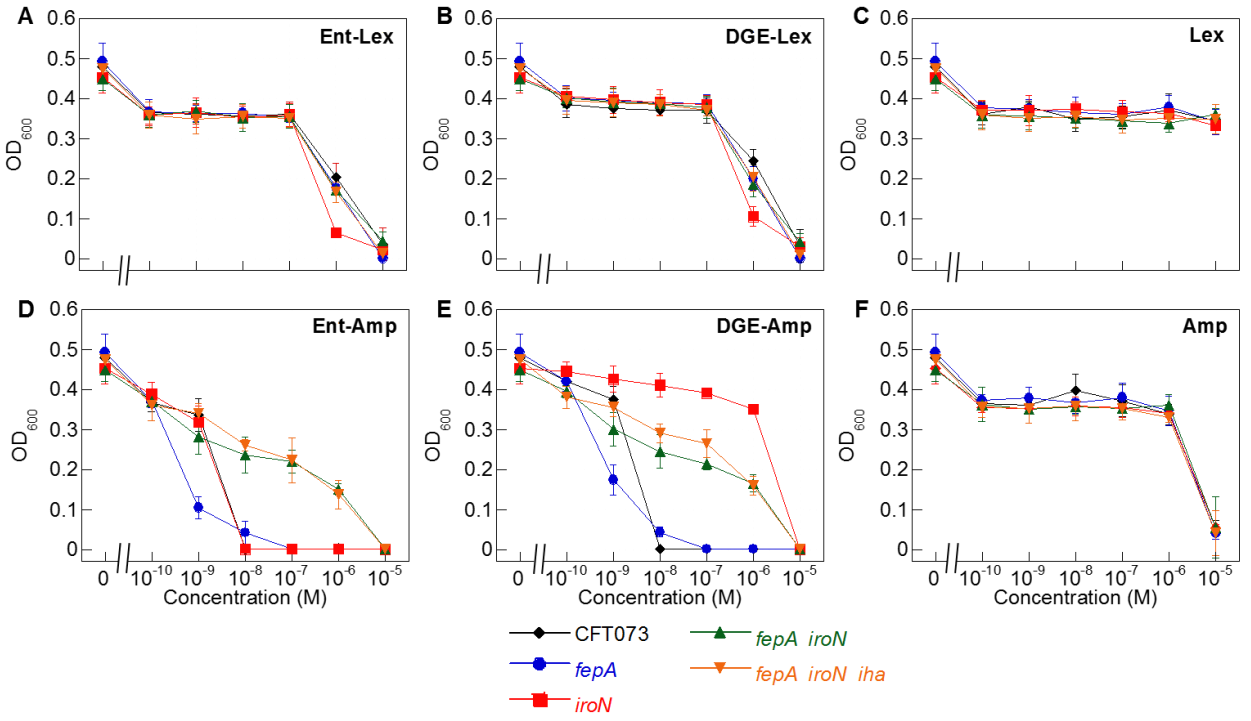

Figure S3. Antibacterial activity of (A) Ent-Lex **3**, (B) DGE-Lex **4**, (C) unmodified Lex and (D) Ent-Amp **1**, (E) DGE-Amp **2** and (F) unmodified Amp against uropathogenic *E. coli* CFT073 and isogenic mutants in the OM receptors *fepA*, *iroN*, *fepA iroN*, and *fepA iroN iha*. All assays were performed in modified M9 medium (20 h, 30°C; mean ± standard deviation, *n* = 3).

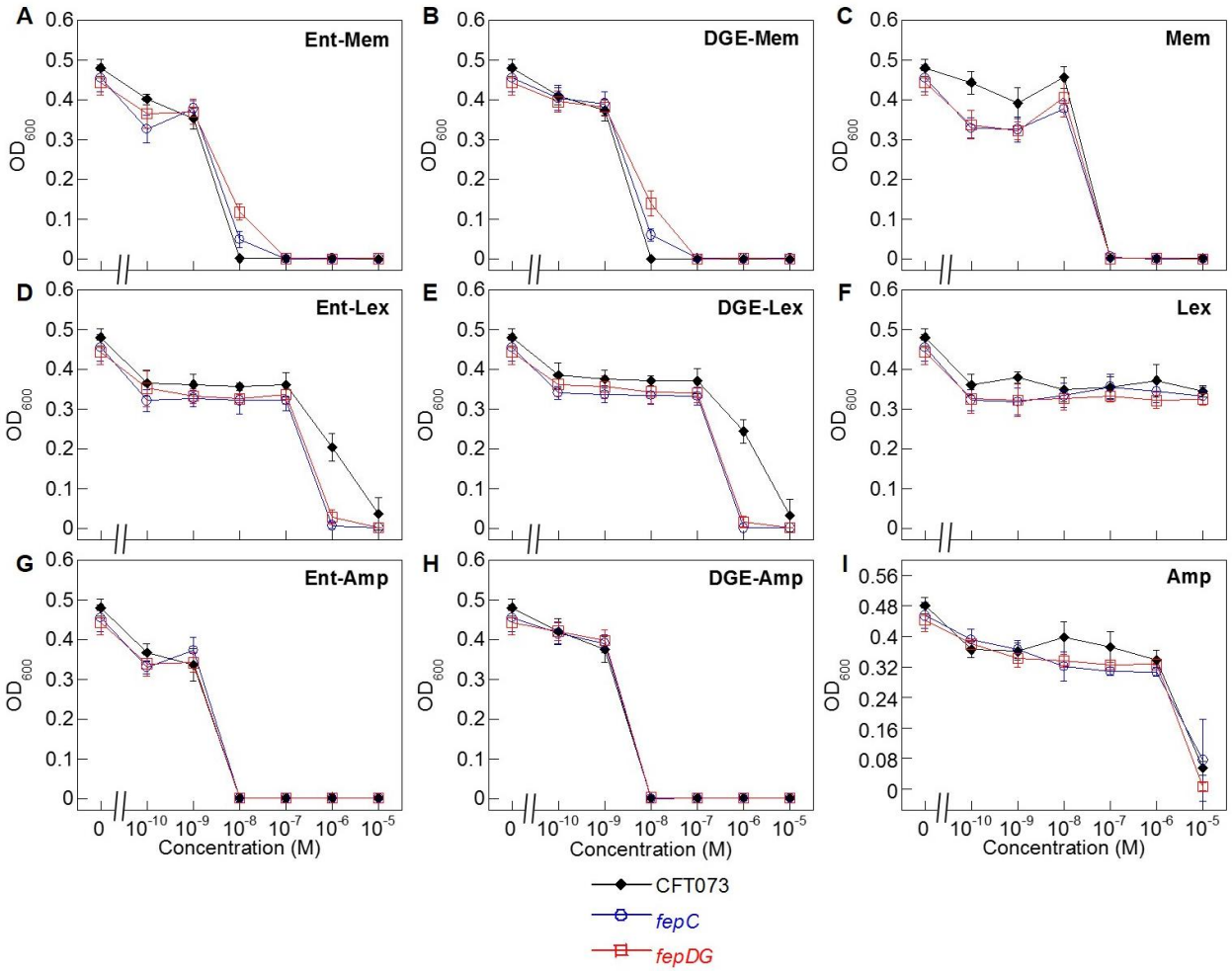

Figure S4. Antibacterial activity of (A, D, G) Ent-β-lactam, (B, E, H) DGE-β-lactam, (C, F, I) unmodified β-lactams against uropathogenic *E. coli* CFT073 and mutants in the IM transporters *fepC* and *fepDG*. All assays were performed in modified M9 medium (20 h, 30°C; mean ± standard deviation, *n* = 3).

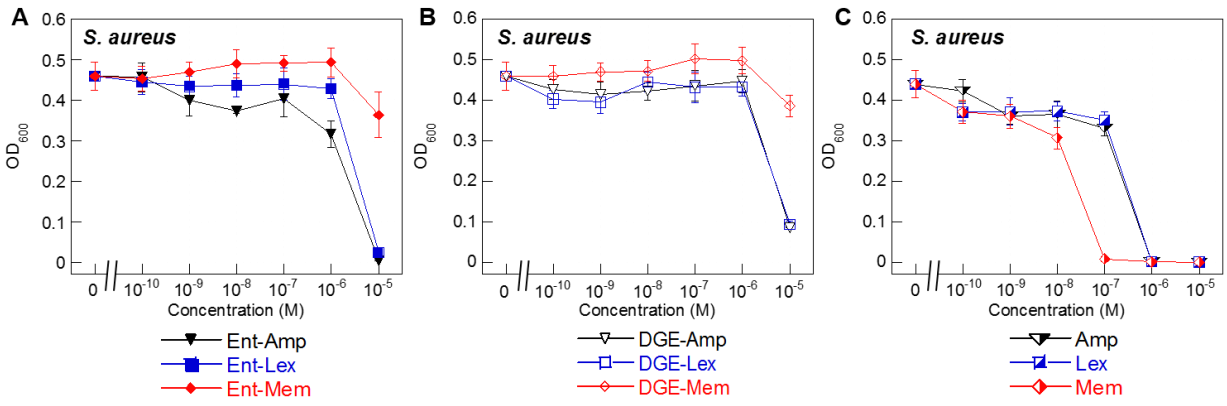

Figure S5. Antibacterial activity of Ent/DGE-β-lactam conjugates **1**-**6** against *S. aureus* ATCC 25923. (A) Activity of Ent-Amp/Lex/Mem **1**, **3**, and **5**; (B) activity of DGE-Amp/Lex/Mem **2**, **4**, and **6**; (C) activity of the parent antibiotics Amp, Lex and Mem. All assays were performed in 50% MHB in the presence of 100 μM Bpy (20 h, 30°C; mean ± standard deviation, *n* = 3).

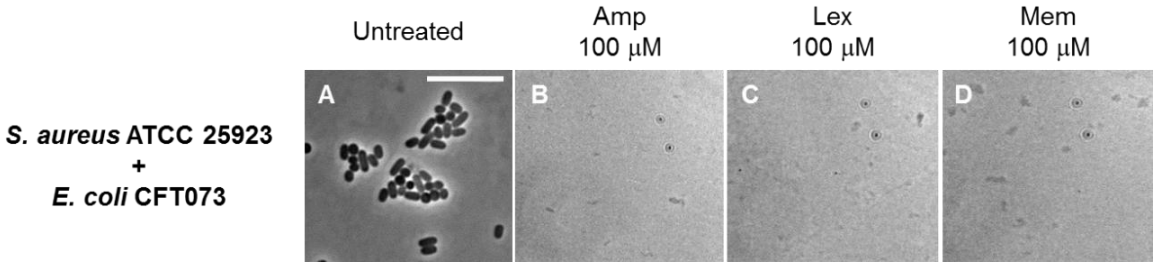

Figure S6. Phase-contrast micrographs of mixed cultures of *E. coli* CFT073 (rods) with *S. aureus* ATCC 25923 (cocci) treated with 100 μM unmodified β-lactams. All cell cultures were incubated with the conjugates in 50% MHB in the presence of 100 μM Bpy for 20 h at 30°C prior the microscopy imaging. Scale bar: 10 μm.

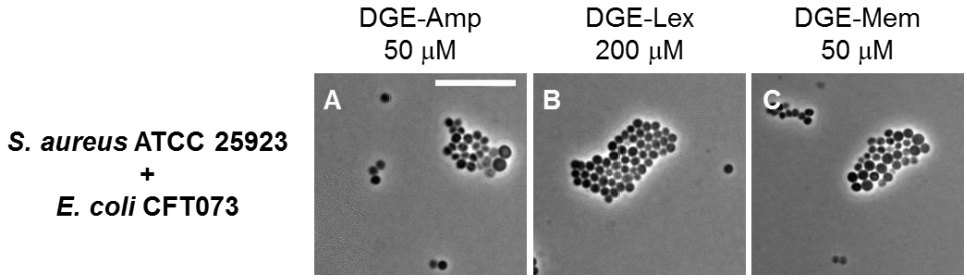

Figure S7. Phase-contrast micrographs of mixed cultures of *E. coli* CFT073 (rods) with *S. aureus* ATCC 25923 (cocci) treated with MIC doses of DGE-β-lactam conjugates. All cell cultures were incubated with the conjugates in 50% MHB in the presence of 100 μM Bpy for 20 h at 30°C prior the microscopy imaging. Scale bar: 10 μm.

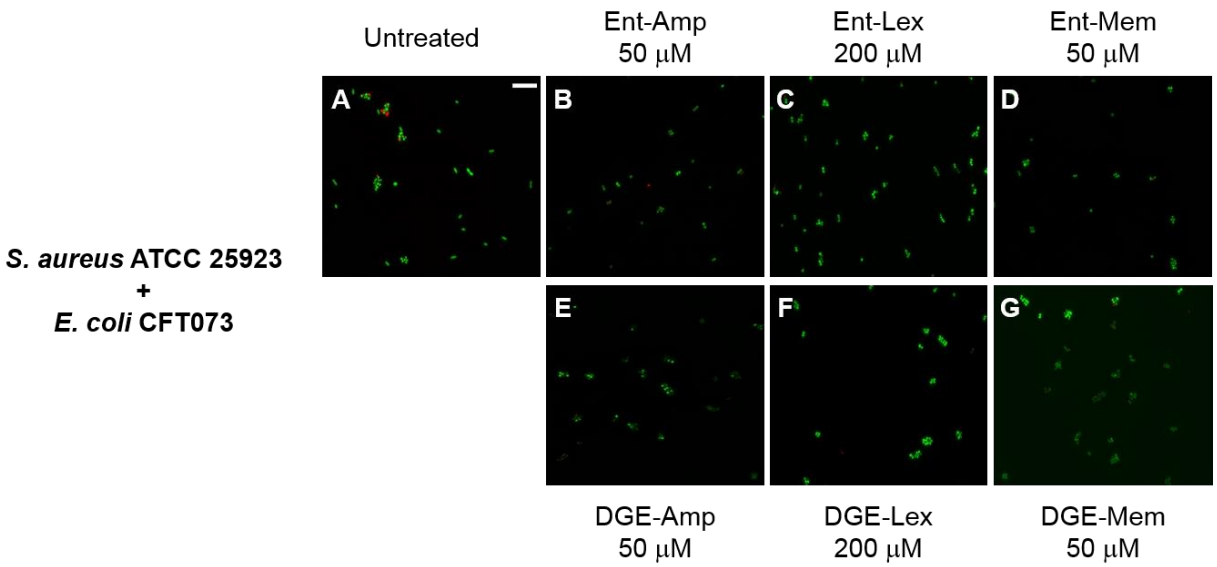

Figure S8. Fluorescence micrographs of mixed cultures of (A) *E. coli* CFT073 (rods) with *S. aureus* ATCC 25923 (cocci) acquired after incubation with the LIVE/DEAD dyes at 30°C for 15 min. The cell cultures were incubated with MIC doses of the (B-D) Ent- or (E-F) DGE-β-lactam conjugates in the presence of 100 μM Bpy for 20 h at 30°C prior to staining. Scale bar: 10 μm. In (C,F) the initial cell density was 10^6 CFU/mL to account for the higher MIC of Ent/DGE-Lex.

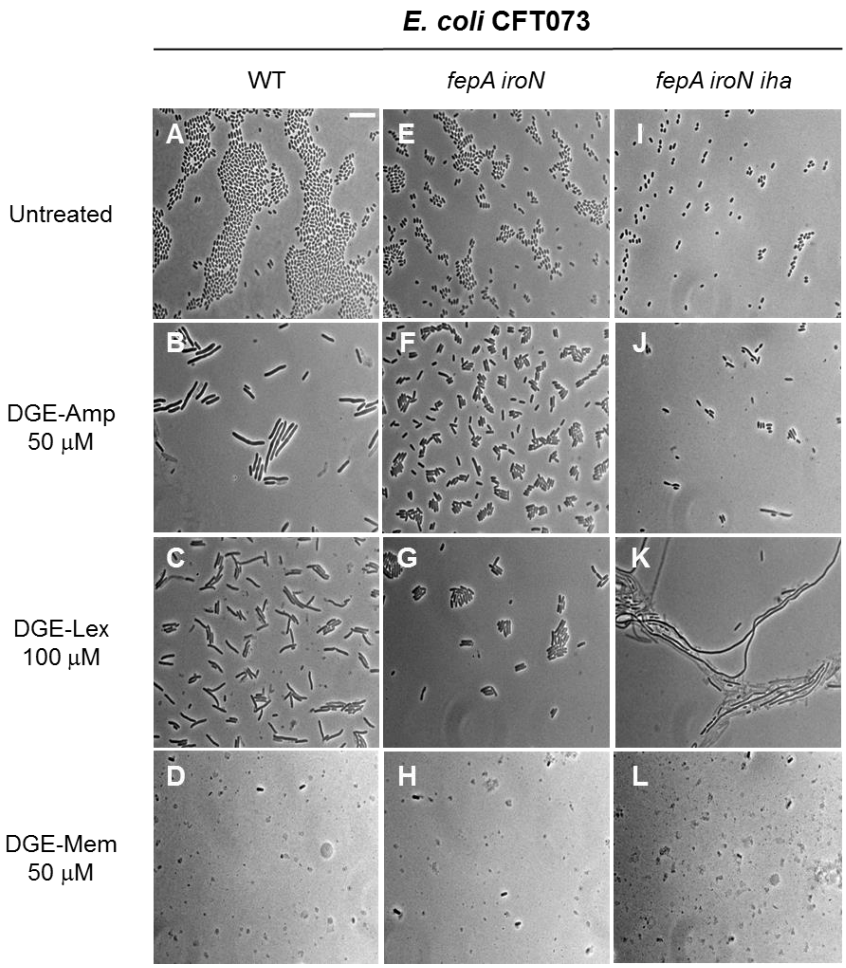

Figure S9. Full-field view micrographs of *E. coli* CFT073 WT (A-D) and the indicated OM receptor mutants (E-L) treated with sub-MIC amounts of DGE-β-lactams in modified M9 medium for 20 h at 30°C. Scale bar: 10 μm.

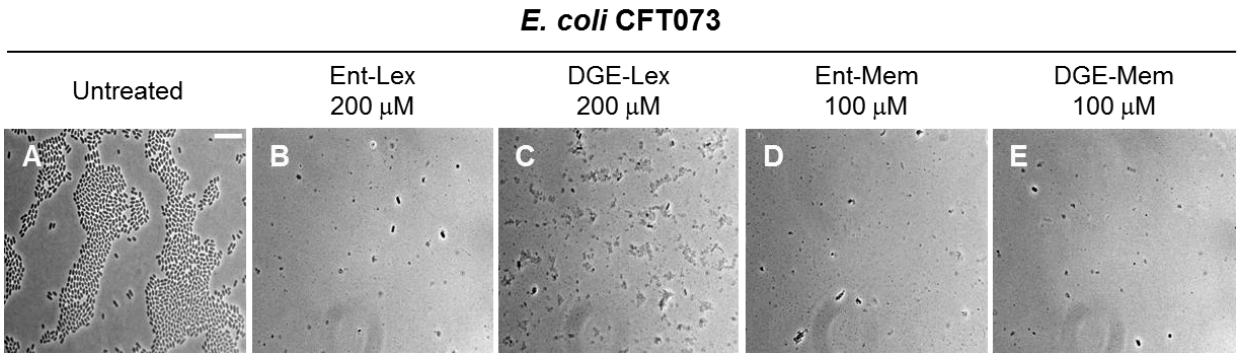

Figure S10. Full-field view micrographs of *E. coli* CFT073 WT treated with MIC amounts of Ent/DGE-Lex/Mem **3-6** in modified M9 medium for 20 h at 30°C. Scale bar: 10 μm. *Note:* initial cell density for B-C was 10^6 CFU/mL to account for higher MIC of Ent/DGE-Lex.

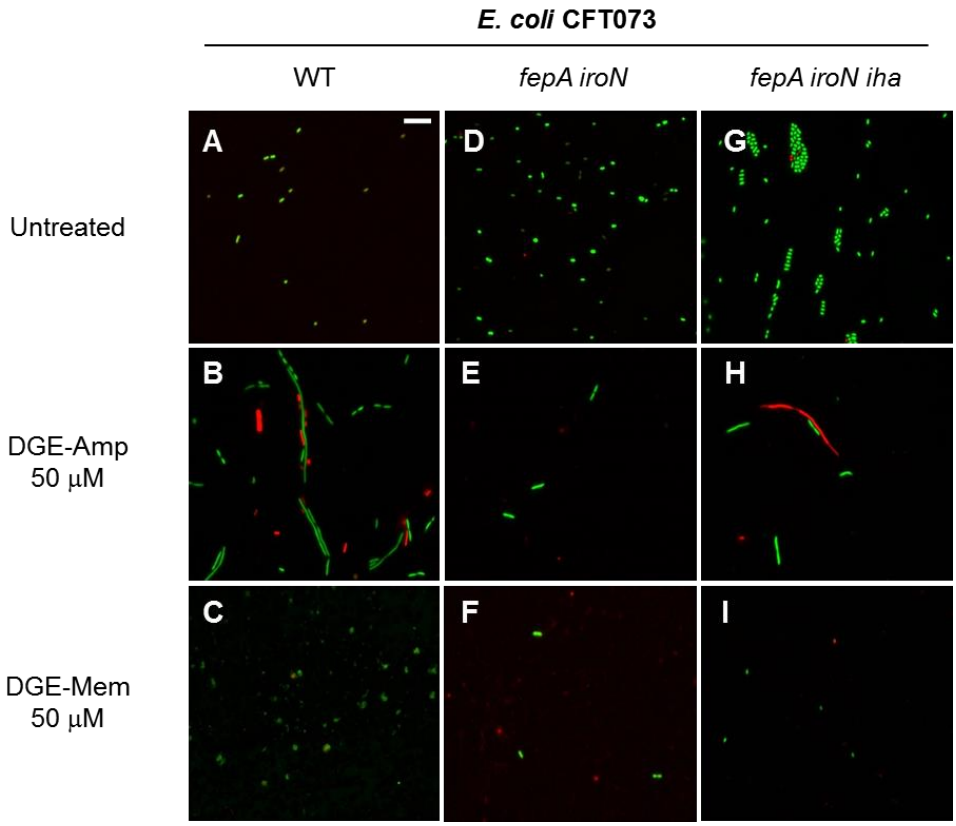

Figure S11. Fluorescence micrographs acquired after incubating *E. coli* CFT073 and the *fepA iroN* and *fepA iroN iha* mutants with the LIVE/DEAD dyes at 30°C for 15 min. The cell cultures were incubated with the DGE conjugates in modified M9 for 20 h at 30°C prior to staining. Scale bar: 10 μm.

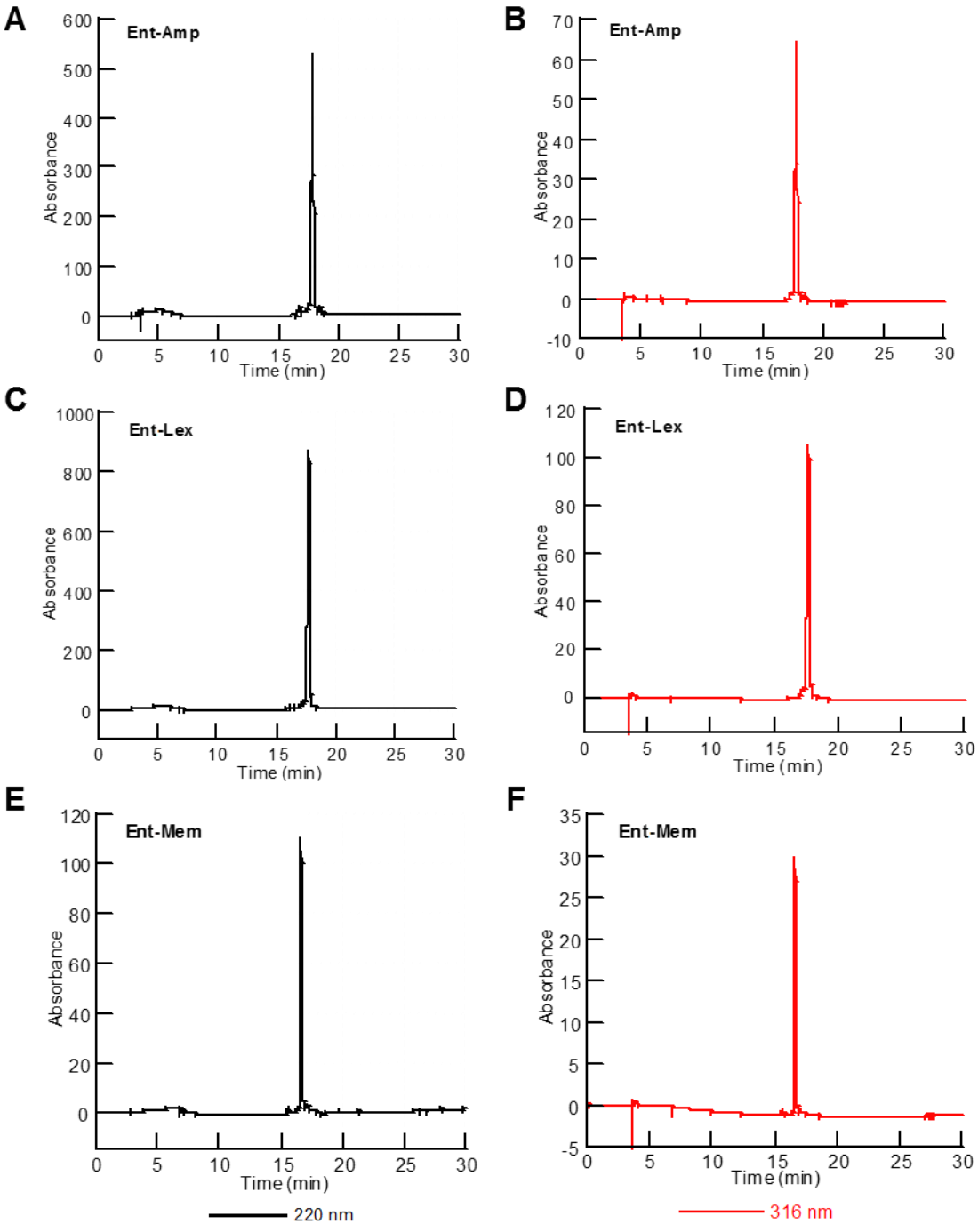

Figure S12. Analytical HPLC traces of purified Ent-Amp (A, B), -Lex (C, D), and -Mem (E, F) (0% B for 5 min followed by 0-100% B over 30 min, 1 mL/min). Absorbance monitored at 220 nm (black) and 316 nm (red). All samples were dissolved in 1:1 v/v/ MeCN/H_2O.

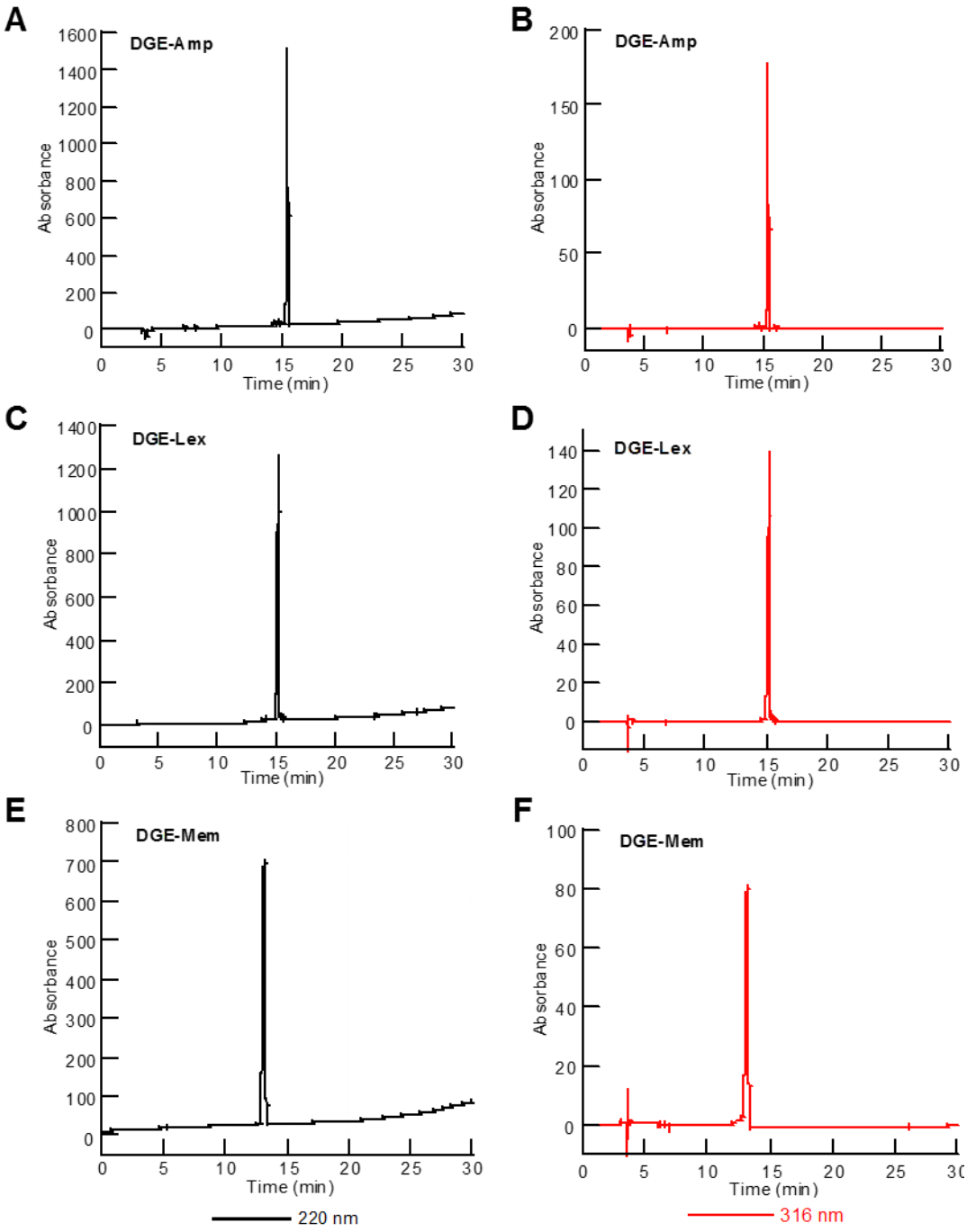

Figure S13. Analytical HPLC traces of purified DGE-Amp (A, B), -Lex (C, D), and -Mem (E, F) (0% B for 5 min followed by 0-100% B over 30 min, 1 mL/min). Absorbance monitored at 220 nm (black) and 316 nm (red). All samples were dissolved in 1:1 v/v/ MeCN/H_2O.

Supplementary References

1 K. A. Datsenko and B. L. Wanner, *Proc. Natl. Acad. Sci. U. S. A.*, 2000, **97**, 6640–6645.
2 J. Frye, J. E. Karlinsey, H. R. Felise, B. Marzolf, N. Dowidar, M. McClelland and K. T. Hughes, *J. Bacteriol.*, 2006, **188**, 2233–2243.
3 T. Baba, T. Ara, M. Hasegawa, Y. Takai, Y. Okumura, M. Baba, K. A. Datsenko, M. Tomita, B. L. Wanner and H. Mori, *Mol. Syst. Biol.*, 2006, **2**, 2006.0008.
4 E. C. Garcia, A. R. Brumbaugh and H. L. T. Mobley, *Infect. Immun.*, 2011, **79**, 1225–1235.
5 T. Zheng and E. M. Nolan, *J. Am. Chem. Soc.*, 2014, **136**, 9677–9691.
6 W. Neumann, M. Sassone-Corsi, M. Raffatellu and E. M. Nolan, *J. Am. Chem. Soc.*, 2018, **140**, 5193–5201.
7 S. L. Chen, C. S. Hung, J. Xu, C. S. Reigstad, V. Magrini, A. Sabo, D. Blasiar, T. Bieri, R. R. Meyer, P. Ozersky, J. R. Armstrong, R. S. Fulton, J. P. Latreille, J. Spieth, T. M. Hooton, E. R. Mardis, S. J. Hultgren and J. I. Gordon, *Proc. Natl. Acad. Sci. U. S. A.*, 2006, **103**, 5977–5982.
8 J. H. Crosa and C. T. Walsh, *Microbiol. Mol. Biol. Rev.*, 2002, **66**, 223–249.
9 M. A. Fischbach, H. Lin, D. R. Liu and C. T. Walsh, *Nat. Chem. Biol.*, 2006, **2**, 132–138.
10 L. D. Loomis and K. N. Raymond, *Inorg. Chem.*, 1991, **30**, 906–911.
11 K. N. Raymond, E. A. Dertz and S. S. Kim, *Proc. Natl. Acad. Sci. U. S. A.*, 2003, **100**, 3584–2588.
12 W. Neumann, A. Gulati and E. M. Nolan, *Curr. Opin. Chem. Biol.*, 2017, **37**, 10–18.
13 E. C. Hagan and H. L. T. Mobley, *Infect. Immun.*, 2007, **75**, 3941–3949.
14 S. Léveillé, M. Caza, J. R. Johnson, C. Clabots, M. Sabri and C. M. Dozois, *Infect. Immun.*, 2006, **74**, 3427–3436.
15 C. J. Alteri and H. L. T. Mobley, *Infect. Immun.*, 2007, **75**, 2679–2688.
16 M. A. Fischbach, H. Lin, L. Zhou, Y. Yu, R. J. Abergel, D. R. Liu, K. N. Raymond, B. L. Wanner, R. K. Strong, C. T. Walsh, A. Aderem and K. D. Smith, *Proc. Natl. Acad. Sci. U. S. A.*, 2006, **103**, 16502–16507.
17 S. I. Müller, M. Valdebenito and K. Hantke, *BioMetals*, 2009, **22**, 691–695.
18 D. H. Goetz, M. A. Holmes, N. Borregaard, M. E. Bluhm, K. N. Raymond and R. K. Strong, *Mol. Cell*, 2002, **10**, 1033–1043.
19 M. Raffatellu, M. D. George, Y. Akiyama, M. J. Hornsby, S. P. Nuccio, T. A. Paixao, B. P. Butler, H. Chu, R. L. Santos, T. Berger, T. W. Mak, R. M. Tsolis, C. L. Bevins, J. V. Solnick, S. Dandekar and A. J. Bäumler, *Cell Host Microbe*, 2009, **5**, 476–486.
20 Y. R. Chan, J. S. Liu, D. A. Pociask, M. Zheng, T. A. Mietzner, T. Berger, T. W. Mak, M. C. Clifton, R. K. Strong, P. Ray and J. K. Kolls, *J. Immunol.*, 2009, **182**, 4947–4956.
21 K. Hantke, G. Nicholson, W. Rabsch and G. Winkelmann, *Proc. Natl. Acad. Sci. U. S. A.*, 2003, **100**, 3677–3682.
22 A. J. Bäumler, R. M. Tsolis, A. W. M. Van Der Velden, I. Stojiljkovic, S. Anic and F. Heffron, *Gene*, 1996, **183**, 207–213.
23 A. J. Bäumler, T. L. Norris, T. Lasco, W. Voigt, R. Reissbrodt, W. Rabsch and F. Heffron, *J. Bacteriol.*, 1998, **180**, 1446–1453.